

Double-Spin Asymmetry in the Cross Section for Exclusive ρ^0 Production in Lepton-Proton Scattering

January 29, 2001

The HERMES Collaboration

A. Airapetian,³¹ N. Akopov,³¹ Z. Akopov,³¹ M. Amarian,^{23,26,31} J. Arrington,² E.C. Aschenauer,⁷
H. Avakian,¹¹ R. Avakian,³¹ A. Avetissian,³¹ E. Avetissian,³¹ P. Bailey,¹⁵ B. Bains,¹⁵ C. Baumgarten,²¹
M. Beckmann,^{12,6} S. Belostotski,²⁴ S. Bernreuther,^{9,29} N. Bianchi,¹¹ H. Böttcher,⁷ A. Borissov,^{6,14,19}
M. Bouwhuis,¹⁵ J. Brack,⁵ S. Brauksiepe,¹² B. Braun,^{9,21} W. Brückner,¹⁴ A. Brüll,¹⁸ P. Budz,⁹
H.J. Bulten,^{17,23,30} G.P. Capitani,¹¹ P. Carter,⁴ P. Chumney,²² E. Cisbani,²⁶ G.R. Court,¹⁶
P.F. Dalpiaz,¹⁰ R. De Leo,³ L. De Nardo,¹ E. De Sanctis,¹¹ D. De Schepper,² E. Devitsin,²⁰
P.K.A. de Witt Huberts,²³ P. Di Nezza,¹¹ V. Djordjadze,⁷ M. Düren,⁹ A. Dvoredsky,⁴ G. Elbakian,³¹
J. Ely,⁵ A. Fantoni,¹¹ A. Fechtchenko,⁸ L. Felawka,²⁸ M. Ferro-Luzzi,²³ K. Fiedler,⁹ B.W. Filippone,⁴
H. Fischer,¹² B. Fox,⁵ J. Franz,¹² S. Frullani,²⁶ Y. Gärber,^{7,9} F. Garibaldi,²⁶ E. Garutti,²³
G. Gavrilov,²⁴ V. Gharibyan,³¹ A. Golendukhin,^{6,21,31} G. Graw,²¹ O. Grebenioun,²⁴ P.W. Green,^{1,28}
L.G. Greeniaus,^{1,28} A. Gute,⁹ W. Haeberli,¹⁷ M. Hartig,²⁸ D. Hasch,^{7,11} D. Heesbeen,²³
F.H. Heinsius,¹² M. Henoch,⁹ R. Hertenberger,²¹ W. Hesselink,^{23,30} G. Hofman,⁵ Y. Holler,⁶
R.J. Holt,^{15,2} B. Hommez,¹³ G. Iarygin,⁸ M. Iodice,²⁶ A. Izotov,²⁴ H.E. Jackson,² A. Jgoun,²⁴ P. Jung,⁷
R. Kaiser,⁷ J. Kanesaka,²⁹ E. Kinney,⁵ A. Kisselev,^{24,2} P. Kitching,¹ H. Kobayashi,²⁹ N. Koch,⁹
K. Königsmann,¹² H. Kolster,^{23,30,18} V. Korotkov,⁷ E. Kotik,¹ V. Kozlov,²⁰ V.G. Krivokhijine,⁸
G. Kyle,²² L. Lagamba,³ A. Laziev,²³ P. Lenisa,¹⁰ T. Lindemann,⁶ W. Lorenzon,¹⁹ N.C.R. Makins,¹⁵
J.W. Martin,¹⁸ H. Marukyan,³¹ F. Masoli,¹⁰ M. McAndrew,¹⁶ K. McIlhany,^{4,18} R.D. McKeown,⁴
F. Meissner,^{7,9,21} F. Menden,¹² A. Metz,²¹ N. Meyners,⁶ O. Mikloukho,²⁴ C.A. Miller,^{1,28} R. Milner,¹⁸
V. Muccifora,¹¹ R. Mussa,¹⁰ A. Nagaitsev,⁸ E. Nappi,³ Y. Naryshkin,²⁴ A. Nass,⁹ K. Negodaeva,⁷
W.-D. Nowak,⁷ K. Oganessyan,¹¹ T.G. O'Neill,² R. Openshaw,²⁸ J. Ouyang,²⁸ B.R. Owen,¹⁵
S.F. Pate,²² S. Potashov,²⁰ D.H. Potterveld,² G. Rakness,⁵ V. Rappoport,²⁴ R. Redwine,¹⁸
D. Reggiani,¹⁰ A.R. Reolon,¹¹ R. Ristinen,⁵ K. Rith,⁹ D. Robinson,¹⁵ A. Rostomyan,³¹ M. Ruh,¹²
D. Ryckbosch,¹³ Y. Sakemi,²⁹ F. Sato,²⁹ I. Savin,⁸ C. Scarlett,¹⁹ A. Schäfer,²⁵ C. Schill,¹² F. Schmidt,⁹
G. Schnell,²² K.P. Schüler,⁶ A. Schwind,⁷ J. Seibert,¹² B. Seitz,¹ T.-A. Shibata,²⁹ T. Shin,¹⁸
V. Shutov,⁸ C. Simani,^{23,30} A. Simon,¹² K. Sinram,⁶ E. Steffens,⁹ J.J.M. Steijger,²³ J. Stewart,^{16,2,28,7}
U. Stösslein,^{7,5} K. Suetsugu,²⁹ M. Sutter,¹⁸ L. Szymanowski,²⁵ S. Taroian,³¹ A. Terkulov,²⁰
O. Teryaev,^{8,25} S. Tessarin,¹⁰ E. Thomas,¹¹ B. Tipton,^{18,4} M. Tytgat,¹³ G.M. Urciuoli,²⁶
J.F.J. van den Brand,^{23,30} G. van der Steenhoven,²³ R. van de Vyver,¹³ J.J. van Hunen,²³
M.C. Vetterli,^{27,28} V. Vikhrov,²⁴ M.G. Vincter,¹ J. Visser,²³ E. Volk,¹⁴ C. Weiskopf,⁹ J. Wendland,^{27,28}
J. Wilbert,⁹ T. Wise,¹⁷ S. Yen,²⁸ S. Yoneyama,²⁹ H. Zohrabian³¹

- ¹Department of Physics, University of Alberta, Edmonton, Alberta T6G 2J1, Canada
²Physics Division, Argonne National Laboratory, Argonne, Illinois 60439-4843, USA
³Istituto Nazionale di Fisica Nucleare, Sezione di Bari, 70124 Bari, Italy
⁴W.K. Kellogg Radiation Laboratory, California Institute of Technology, Pasadena, California 91125, USA
⁵Nuclear Physics Laboratory, University of Colorado, Boulder, Colorado 80309-0446, USA
⁶DESY, Deutsches Elektronen Synchrotron, 22603 Hamburg, Germany
⁷DESY Zeuthen, 15738 Zeuthen, Germany
⁸Joint Institute for Nuclear Research, 141980 Dubna, Russia
⁹Physikalisches Institut, Universität Erlangen-Nürnberg, 91058 Erlangen, Germany
¹⁰Istituto Nazionale di Fisica Nucleare, Sezione di Ferrara and Dipartimento di Fisica, Università di Ferrara, 44100 Ferrara, Italy
¹¹Istituto Nazionale di Fisica Nucleare, Laboratori Nazionali di Frascati, 00044 Frascati, Italy
¹²Fakultät für Physik, Universität Freiburg, 79104 Freiburg, Germany
¹³Department of Subatomic and Radiation Physics, University of Gent, 9000 Gent, Belgium
¹⁴Max-Planck-Institut für Kernphysik, 69029 Heidelberg, Germany
¹⁵Department of Physics, University of Illinois, Urbana, Illinois 61801, USA
¹⁶Physics Department, University of Liverpool, Liverpool L69 7ZE, United Kingdom
¹⁷Department of Physics, University of Wisconsin-Madison, Madison, Wisconsin 53706, USA
¹⁸Laboratory for Nuclear Science, Massachusetts Institute of Technology, Cambridge, Massachusetts 02139, USA
¹⁹Randall Laboratory of Physics, University of Michigan, Ann Arbor, Michigan 48109-1120, USA
²⁰Lebedev Physical Institute, 117924 Moscow, Russia
²¹Sektion Physik, Universität München, 85748 Garching, Germany
²²Department of Physics, New Mexico State University, Las Cruces, New Mexico 88003, USA
²³Nationaal Instituut voor Kernfysica en Hoge-Energiefysica (NIKHEF), 1009 DB Amsterdam, The Netherlands
²⁴Petersburg Nuclear Physics Institute, St. Petersburg, Gatchina, 188350 Russia
²⁵Institut für Theoretische Physik, Universität Regensburg, 93040 Regensburg, Germany
²⁶Istituto Nazionale di Fisica Nucleare, Sezione Roma1-Gruppo Sanità and Physics Laboratory, Istituto Superiore di Sanità, 00161 Roma, Italy
²⁷Department of Physics, Simon Fraser University, Burnaby, British Columbia V5A 1S6, Canada
²⁸TRIUMF, Vancouver, British Columbia V6T 2A3, Canada
²⁹Department of Physics, Tokyo Institute of Technology, Tokyo 152, Japan
³⁰Department of Physics and Astronomy, Vrije Universiteit, 1081 HV Amsterdam, The Netherlands
³¹Yerevan Physics Institute, 375036, Yerevan, Armenia

Abstract

Evidence for a positive longitudinal double-spin asymmetry $\langle A_1^p \rangle = 0.24 \pm 0.11_{\text{stat}} \pm 0.02_{\text{syst}}$ in the cross section for exclusive diffractive $\rho^0(770)$ vector meson production in polarised lepton-proton scattering was observed by the HERMES experiment. The longitudinally polarised 27.56 GeV HERA positron beam was scattered off a longitudinally polarised pure hydrogen gas target. The average invariant mass of the photon-proton system has a value of $\langle W \rangle = 4.9$ GeV, while the average negative squared four-momentum of the virtual photon is $\langle Q^2 \rangle = 1.7$ GeV². The ratio of the present result to the corresponding spin asymmetry in inclusive deep-inelastic scattering is in agreement with an early theoretical prediction based on the generalised vector meson dominance model.

PACS numbers : 13.25.-k; 13.40.-f; 13.60.-r; 13.60.Le; 13.88.+e; 14.40.Cs

Keywords : Lepton-Nucleon Scattering, Rho Production, Asymmetries, Photoabsorbtion.

Diffractive ρ^0 production in lepton-nucleon scattering is often described as the fluctuation of the virtual photon emitted by the lepton into an intermediate virtual $q\bar{q}$ state or off-shell ρ^0 meson. This intermediate state is scattered onto the mass shell by a diffractive strong interaction with the target, leaving the target nucleon intact [1]. Several competing models for this process are schematically shown in the graphs of Figure 1. At low energy the ρ^0 cross section shows a strong decrease with increasing energy [2–4], which can be described by the exchange of Reggeons. At an invariant mass of the photon-nucleon system of approximately $W = 5$ GeV (see below for definitions of all kinematic variables), the cross section exhibits a dramatic change from a rapidly falling to a weakly rising W -dependence [5, 6]. Above this energy, models of the interaction based on Regge theory involve the exchange of Pomerons. Alternatively, there exist perturbative QCD calculations of vector-meson production by longitudinal photons that are based on the exchange of quarks and gluons and on the non-perturbative description of nucleon structure in terms of skewed parton distributions [7–10]. Both types of models — Regge theory and pQCD calculations — have achieved some degree of success in reproducing the observed unpolarised cross sections for ρ^0 production [6, 11, 12]. It has been shown that in the HERMES kinematic range, the data for exclusive ρ^0 production by longitudinal photons can be described by a pQCD calculation that includes a combination of both quark and gluon exchange mechanisms [6].

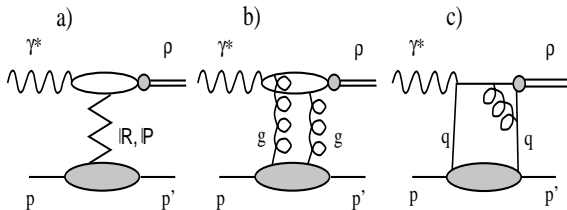


Figure 1: Schematic graphs for various models of exclusive diffractive ρ^0 production: a) Reggeon or Pomeron exchange in models based on Regge theory, b) two-gluon exchange and c) quark exchange in models inspired by perturbative QCD.

Previously, the spin dependence of the ρ^0 lepton-production process has been investigated by measuring the angular distributions of the production and the self-analysing $\rho^0 \rightarrow \pi^+\pi^-$ decay. Spin degrees of freedom in the cross section can be described by spin density matrix elements constructed from helicity-conserving and non-conserving amplitudes for particle exchange in the t -channel [13]. Experiments have shown that the helicity of the photon in the γ^*N centre-of-mass system is approximately retained by the ρ^0 meson, a phenomenon known as s -channel helicity conservation (SCHC), and that the exchanged object has natural parity $(-1)^L$ [2], which can be associated with *e.g.* Reggeon and Pomeron exchange. Typically, the initial spin states of the target nucleon were averaged and the final spin states were summed [13], since they were experimentally inaccessible. The general case where the initial spin states of a longitudinally polarised beam and a longitudinally or transversely polarised target are explicitly included in the formalism of spin density matrix elements has been discussed in Ref. [14].

Up to now, little attention has been paid to the theoretical prediction of double-spin asymmetries in the cross section for diffractive processes, i.e. to the dependence of the cross section on the product of the initial polarisations of beam *and* target; usually a double-spin asymmetry of zero was assumed for ρ^0 production. Nevertheless, there exists early work where spin asymmetries are given by the ratio of helicity-conserving amplitudes of unnatural to natural parity exchange in the t -channel; this work is based on the formalism of spin density matrix elements and the generalised vector meson dominance model (GVMD) [15] which describes the hadronic fluctuation of the virtual photon as a coherent superposition of vector meson states and the transitions between them. In particular, the longitudinal double-spin asymmetry in exclusive ρ^0 production was predicted to be about twice as large as the corresponding asymmetry in inclusive deep-inelastic scattering (DIS) [16].

No published prediction based on perturbative QCD calculations exists for double-spin asymmetries in the photo- or lepto-production of ρ^0 mesons. Polarised quasi-real J/ψ photoproduction involving the exchange of two gluons was dis-

cussed in Ref. [17]. However, because this calculation relies on the heavy quark approximation, the relevant physics for this process is qualitatively different and no direct implications for exclusive ρ^0 production in the HERMES kinematic range can be drawn.

This paper presents the first observation of a non-zero longitudinal double-spin asymmetry in the cross section for exclusive $\rho^0(770)$ meson production in polarised lepton-nucleon scattering. This observable was measured by the HERMES experiment [18] in the years 1996 and 1997.

The HERMES experiment uses the polarised 27.56 GeV positron beam of the HERA storage ring. A transverse polarisation of the positron beam develops through an asymmetry in the small spin-flip amplitudes for synchrotron radiation in the bending dipoles — the Sokolov-Ternov effect [19]. Longitudinal beam polarisation is achieved by spin rotators in front and behind the experiment. Typical beam polarisation values are between 0.5 to 0.6, measured with a negligible statistical uncertainty and a systematic uncertainty of 0.02 [20].

In the years 1996 and 1997 a longitudinally polarised internal atomic hydrogen gas target was used [21]. The orientation of the target polarisation is randomly selected about once per minute. The average target polarisation for the combined 1996 and 1997 data on the polarised hydrogen target is 0.88 ± 0.05 , where the uncertainty is predominantly systematic.

The forward magnetic spectrometer [18] is divided into symmetric upper and lower halves by the positron and the (unused) proton beam lines. The acceptance covers $40 < |\theta_v| < 140$ mrad in the vertical direction and $|\theta_h| < 170$ mrad in the horizontal direction. Over the kinematic range of the experiment, the momentum resolution for positrons is 0.7-1.3% and the uncertainty in the scattering angle is about 0.6 mrad. Positrons are distinguished from hadrons by four sub-systems for particle identification: a lead-glass electromagnetic calorimeter, a preshower detector, a transition-radiation detector, and a threshold Čerenkov detector. The positron identification has an efficiency of better than 98% at a hadron contam-

ination of less than 1% over the kinematic range of the experiment. The relative luminosity for the two target spin states is measured by counting coincident e^+e^- pairs from elastic (Bhabha) scattering of the beam positrons off the electrons of the target gas atoms. The present data correspond to an integrated luminosity of about 55 pb^{-1} .

At HERMES energies, the lepton-nucleon interaction is mediated by a virtual photon with negative 4-momentum squared $Q^2 \equiv -q^2 \equiv -(k - k')^2 \sim 4EE' \sin^2(\theta/2)$, where $k(E)$ and $k'(E')$ denote the four-momenta (energies) of the incoming and outgoing lepton and θ is the polar scattering angle of the lepton. The target nucleons are at rest: $p = (M, \vec{0})$. The invariant mass W of the photon-nucleon system is given by $W^2 \equiv (q + p)^2 \stackrel{lab}{=} M^2 + 2M\nu - Q^2$. Here, $\nu \equiv p \cdot q/M = E - E'$ denotes the photon energy in the target rest frame and $y \equiv \nu/E$ the fractional photon energy. The Björken scaling variable is defined as $x = Q^2/2M\nu$. In diffractive ρ^0 production, the photon-nucleon cross section falls exponentially with the squared four-momentum transfer to the target $t \equiv (q - v)^2 < 0$, with v the four-momentum of the ρ^0 meson. At t_0 , the maximum (least negative) value of t kinematically allowed for fixed Q^2 , ν , M_Y , and $M_{\pi\pi}$, the momentum of the final state ρ^0 meson is parallel to the direction of the incoming photon in the photon-nucleon centre-of-mass system. Here, M_Y is the invariant mass of the undetected final state and $M_{\pi\pi} = \sqrt{v^2}$ is the reconstructed invariant mass of the ρ^0 candidate. The squared four-momentum transfer t' beyond t_0 is given by $t' \equiv t - t_0 < 0$. In order to select exclusive diffractive events, the excitation energy ΔE transferred to the target nucleon can be used as a measure of exclusivity: $\Delta E \equiv (M_Y^2 - M^2)/2M \stackrel{lab}{=} \nu - E_\rho + t/2M$, with E_ρ the energy of the ρ^0 meson. In the case of an exclusive process, no energy is transferred to the target ($\Delta E \cong 0$), and the target nucleon stays intact ($p'^2 = p^2$).

Three angles Φ , ϕ , and θ are necessary for a complete description of the angular distribution of the ρ^0 meson production and decay [13]. The azimuthal production angle Φ is the angle between

the lepton scattering plane and the ρ^0 meson production plane in the photon-nucleon centre-of-mass frame. The ρ^0 decay is described in the ρ^0 meson rest frame by two angles: i) the azimuthal angle ϕ between the production and the decay plane and ii) the polar angle θ of the positively charged decay particle with respect to the z -axis of the ρ^0 meson rest frame, which is defined opposite to the direction of the scattered nucleon.

In the exclusive process $ep \rightarrow ep\rho^0$, only the scattered positron and the $\rho^0 \rightarrow \pi^+\pi^-$ decay products are detected at HERMES, since the recoiling target proton remains outside of the spectrometer acceptance. Consequently, as a first step, only events were selected with exactly three tracks — a positron and two oppositely charged hadrons. The tracks are required to be within the nominal spectrometer acceptance and to originate from a common vertex in the target region. To ensure that the trigger efficiency is close to unity, a minimum energy of the scattered positron above the calorimeter threshold of the trigger is required.

The ρ^0 candidates are selected within the range $0.62 < M_{\pi\pi} < 0.92$ GeV of the reconstructed invariant mass of the hadron pair. The requirement $-t' < 0.4$ GeV² suppresses non-diffractive processes, which fall off more slowly with $-t'$ than diffractive ρ^0 production. Exclusive events appear as a peak near zero in the excitation energy distribution shown in Fig. 2; the shaded area $|\Delta E| < 0.6$ GeV indicates the events used for analysis. For $\Delta E \gtrsim 2$ GeV the spectrum is dominated by background from non-exclusive processes where, for example, energy is absorbed by the target. After all selection criteria were applied, about 2800 exclusive ρ^0 events remained from the combined 1996 and 1997 data on the polarised hydrogen target. The average values of the relevant kinematic variables are $\langle W \rangle = 4.9$ GeV, $\langle Q^2 \rangle = 1.7$ GeV², $\langle -t' \rangle = 0.1$ GeV², $\langle x \rangle = 0.07$. HERMES results on the cross section for exclusive ρ^0 production and spin density matrix elements as well as distributions of the invariant mass, t' and other kinematic variables can be found in Refs. [6,22,27].

The predominant contribution to the background from non-exclusive processes is combinatorial hadronic background from deep-inelastic scat-

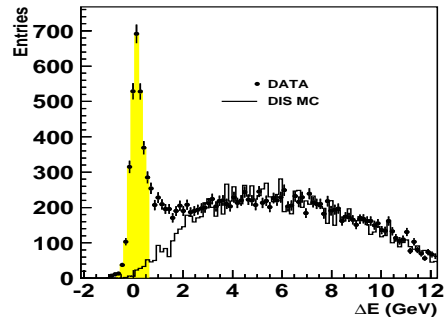


Figure 2: Distribution in the excitation energy ΔE for the decay channel $\rho^0 \rightarrow \pi^+\pi^-$, after all other event selection criteria were applied. The histogram is a Monte Carlo simulation of combinatorial background from deep-inelastic scattering (DIS). The shaded area indicates the events that were used for the analysis.

tering events. In the region of the exclusive peak (shaded area in Fig. 2), it is not separable on an event-by-event basis. It is subtracted using a Monte Carlo simulation based on the LEPTO [23] generator and the LUND fragmentation model [24]. The Monte Carlo events are subject to the ρ^0 event selection criteria yielding the ΔE distribution shown by the histogram in Fig. 2; it is normalised to the data in the region $\Delta E > 3$ GeV. The contamination in the ρ^0 data sample within the signal region $|\Delta E| < 0.6$ GeV is typically less than 10%. For the asymmetry analysis, the background was subtracted separately for each spin state and kinematic bin, accounting for the asymmetry contribution from DIS background. The statistical uncertainty in this background correction is propagated into the statistical uncertainty of the measured asymmetry.

An additional contribution to the non-exclusive background arises from double-diffractive production of ρ^0 . This process is similar to the exclusive process of interest, except that the proton target is dissociated. Based on previous measurements [25], the contribution of this background was estimated [6] to be less than $6 \pm 2\%$ within the stringent $|\Delta E| < 0.6$ GeV requirement.

Background from exclusive processes includes the contributions of non-resonant pion pair production and of the decay $\omega(783) \rightarrow \pi^+\pi^-$ (branch-

ing ratio 2.2%). These two processes contribute less than 1% to the signal region; for the present analysis both contributions remain within the data sample. Mis-reconstructed ϕ meson decays $\phi \rightarrow K^+K^-$ appear at $M_{\pi\pi}$ below 0.6 GeV, and are excluded by the invariant mass requirement.

In lepton-nucleon scattering, with both target and beam longitudinally polarised, the experimentally accessible lepton-nucleon cross section asymmetry A_{\parallel} is defined in terms of $\sigma^{\vec{\zeta}}$ and $\sigma^{\overleftarrow{\zeta}}$, the cross sections for parallel and anti-parallel orientation of the target polarisation with respect to the direction of the beam polarisation:

$$A_{\parallel} \equiv \frac{\sigma^{\overleftarrow{\zeta}} - \sigma^{\vec{\zeta}}}{\sigma^{\overleftarrow{\zeta}} + \sigma^{\vec{\zeta}}} = \frac{N^{\overleftarrow{\zeta}}L^{\overleftarrow{\zeta}} - N^{\vec{\zeta}}L^{\vec{\zeta}}}{N^{\overleftarrow{\zeta}}L^{\overleftarrow{\zeta}} + N^{\vec{\zeta}}L^{\vec{\zeta}}}. \quad (1)$$

It is determined from the number of events $N^{\vec{\zeta}(\overleftarrow{\zeta})}$ per beam and target spin configuration, weighted with the relative luminosities of each spin configuration $L^{\vec{\zeta}(\overleftarrow{\zeta})}$ and $L_P^{\vec{\zeta}(\overleftarrow{\zeta})}$. Here, $L_P^{\vec{\zeta}(\overleftarrow{\zeta})} = \langle L|p_B p_T| \rangle^{\vec{\zeta}(\overleftarrow{\zeta})}$ is the relative luminosity weighted with the product of beam and target polarisation. For the HERMES pure hydrogen gas target, no dilution from other material exists. The statistical uncertainty of A_{\parallel} is determined by the event statistics; the small statistical uncertainties of the luminosity and the polarisation measurements are included in the systematic uncertainty.

The spin dependence of the photon-nucleon interaction is characterised by two asymmetries of the interaction cross section for virtual photons: i) the asymmetry A_1 for a transverse photon with well defined helicity interacting with a longitudinally polarised target nucleon and ii) the asymmetry A_2 , which arises from the interference between transverse and longitudinal photons. Specifically,

$$A_1 = \frac{\sigma_{1/2} - \sigma_{3/2}}{\sigma_{1/2} + \sigma_{3/2}} \quad \text{and} \quad A_2 = \frac{\sigma_{LT}}{\sigma_{1/2} + \sigma_{3/2}}. \quad (2)$$

Here $\sigma_{3/2}$ and $\sigma_{1/2}$ denote the virtual-photon interaction cross sections, with 3/2 and 1/2 the projection of the total spin of the photon-nucleon system along the photon momentum, and $\sigma_{LT} = \sqrt{\sigma_L \cdot \sigma_T}$ is the interference cross section between longitudinal and transverse photons. The definitions of A_1 and A_2 are formally independent of

the physics process that the virtual photon undergoes. Note that in inclusive DIS, A_1 and A_2 can be interpreted in terms of the polarised structure functions g_1 and g_2 .

The measured asymmetry A_{\parallel} is related to the photon-nucleon interaction asymmetries A_1 and A_2 by

$$A_{\parallel} = D \cdot (A_1 + \eta A_2). \quad (3)$$

The effective polarisation D of the virtual photon is given by

$$D = \frac{1 - (1-y)\epsilon}{1 + \epsilon R} \quad \text{and} \quad \epsilon \simeq \frac{1 - y - \frac{Q^2}{4E^2}}{1 - y + \frac{y^2}{2} + \frac{Q^2}{4E^2}}, \quad (4)$$

with $\epsilon = \Gamma_L/\Gamma_T$ the ratio of fluxes and $R = \sigma_L/\sigma_T$ the ratio of the reaction cross sections for longitudinal and transverse photons. The kinematic factor η in Eq. 3 is given by $\eta = 2\epsilon\sqrt{Q^2}/\{(M + 2E)[1 - (1-y)\epsilon]\}$.

In exclusive ρ^0 production, the ratio R can be measured via the angular distributions of the ρ^0 decay; it shows a strong increase with Q^2 , becoming larger than unity¹ at $Q^2 \geq 3$ GeV². From a fit to HERMES data [27], a parameterisation of R in the form

$$R(Q^2) = c_0(W) \left[\frac{Q^2}{m_\rho^2} \right]^{c_1} \quad (5)$$

with parameters $c_0 = 0.32$ and $c_1 = 0.66$ was obtained. This parameterisation yields for the present exclusive ρ^0 data sample an average value of $D = 0.4$ at an average value of $R = 0.62$. From the value of R follows that the contributions of longitudinal and transverse photons to ρ^0 production at HERMES are about equally important; however, as longitudinal photons have zero helicity, the asymmetry A_1^{ρ} discussed here can arise only from transverse photons.

In inclusive deep-inelastic scattering, the asymmetry A_2 was measured using a transversely polarised target to be positive but close to zero [28, 29]. In contrast, in ρ^0 production information about A_2^{ρ} is available through the measurement of angular distributions of the decay pions. For $W \gtrsim 3$ GeV, the interference cross section σ_{LT} is

¹For comparison, the ratio R in inclusive DIS has a flat distribution and varies between 0.2 and 0.4 [26, 28].

maximal, since the phase difference between amplitudes for ρ^0 production from transverse and longitudinal photons was measured to be small [27]. The contribution of A_2^ρ to A_{\parallel}^ρ is then given by the positivity limit $A_2^\rho = \sqrt{R(Q^2)}$. It is suppressed by the small kinematic factor η , which has an average value $\langle \eta \rangle = 0.06$ for the exclusive ρ^0 data sample.

The photon-nucleon asymmetry A_1^ρ in a given kinematic bin is obtained from the experimental lepton-nucleon asymmetry A_{\parallel}^ρ using Eq. 3:

$$A_1^\rho = \frac{A_{\parallel}^\rho}{\langle D \rangle} - \langle \eta \sqrt{R(Q^2)} \rangle, \quad (6)$$

where $\langle D \rangle$ and $\langle \eta \sqrt{R(Q^2)} \rangle$ are the average values for all events in the bin.

The stability of the observed asymmetry was studied by varying the event selection requirements and comparing alternative methods of background subtraction [30]. These systematic studies were performed for both the experimental asymmetry A_{\parallel}^ρ and for the photon-nucleon asymmetry A_1^ρ . No significant dependence on the event selection criteria was observed during variation of requirements on vertex geometry, particle identification and event kinematics. Using the DIS Monte Carlo simulation, a contribution of DIS background to the asymmetry A_{\parallel}^ρ of 0.003 was found, and taken as an upper limit on the associated systematic uncertainty. Two alternative techniques of background subtraction produced similar results: one based on events at high values of $-t'$ where the non-exclusive background dominates the data [22], and another using an empirical fit to the elastic peak in the ΔE distribution. The quoted asymmetries and the bin centers have not been corrected for the limited acceptance of the spectrometer for ρ^0 production; resolution effects and bin-to-bin smearing can be neglected due to the large bin size in the present analysis. A comparison of the 1996 and 1997 data sets with opposite beam helicities yielded consistent results, excluding possible contributions from single-spin asymmetries. The contribution of electroweak radiative processes to the measured asymmetry is expected to be negligible [31]. The uncertainties in the beam and target polarisation measurements cause a 6.6% fractional systematic uncertainty in the asymmetries.

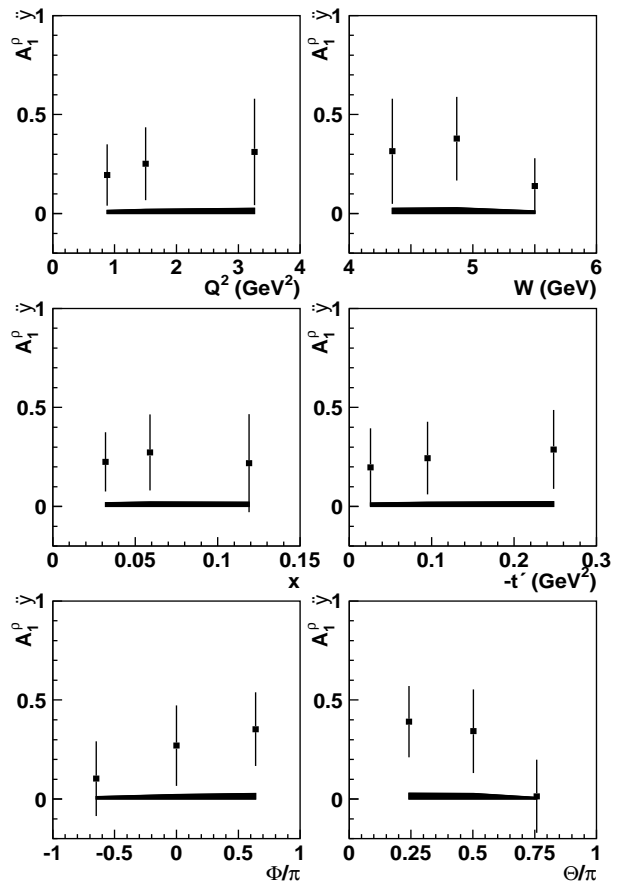


Figure 3: Photon-nucleon asymmetry A_1^ρ in exclusive ρ^0 production versus Q^2 , W , x , $-t'$, Φ , and θ . Error bars and error bands denote the statistical and experimental systematic uncertainties, respectively.

Evidence for a positive double-spin asymmetry has been observed in the lepton-nucleon cross section for exclusive ρ^0 production on the longitudinally polarised hydrogen target. Averaged over the kinematic acceptance, the measured asymmetry has a value of

$$\langle A_{\parallel}^\rho \rangle = 0.119 \pm 0.045_{\text{stat}} \pm 0.008_{\text{syst}}, \quad (7)$$

where the systematic uncertainty is dominated by the contributions from the beam and target polarisation measurements. Using the average depolarisation factor $\langle D \rangle = 0.40$, the average photon-

nucleon asymmetry A_1^ρ was found according to Eq. 6

$$\langle A_1^\rho \rangle = 0.24 \pm 0.11_{\text{stat}} \pm 0.02_{\text{syst}}, \quad (8)$$

where a contribution $\langle \eta\sqrt{R} \rangle = 0.053$ by the asymmetry A_2^ρ was subtracted.

Fig. 3 shows the dependence of A_1^ρ on the kinematic variables Q^2 , W , x , $-t'$, and the angles Φ and θ . Error bars denote the statistical uncertainties and the dark band at the bottom of the plots indicates the systematic uncertainty. Within the statistical uncertainty of the measurement, no significant dependence on any of the kinematic variables or angles can be seen in either A_{\parallel}^ρ or in A_1^ρ .

The present result for A_1^ρ is compared to the already mentioned theoretical prediction [16], which is based on the description of diffractive exclusive ρ^0 leptonproduction *and* inclusive deep-inelastic scattering by the GVMD. At $x < 0.2$, this model can relate the asymmetry for exclusive ρ^0 production A_1^ρ to the asymmetry $A_1^{\gamma^*p}$ for inclusive DIS at the same value of x . Assuming an *approximate* validity of SCHC, spin asymmetries were written as the ratio of helicity-conserving amplitudes of unnatural $(-1)^{L+1}$ to natural $(-1)^L$ parity exchange in the t -channel. A non-zero asymmetry indicates a contribution of exchange processes with unnatural parity to the *interference* responsible for the asymmetry. This contribution may be large enough to yield an asymmetry while remaining negligible in the *incoherent sum* of squared amplitudes for the cross section that was observed to be dominated by natural parity exchange in measurements of angular distributions in ρ^0 production and decay [27]. Such an unnatural parity exchange is consistent with an exchange of diquark objects as they can have both natural and unnatural parity. Quark exchange has been shown to be the predominant contribution in exclusive ρ^0 production by longitudinal photons at HERMES energies [6]; the present result suggests that diquark exchange may also contribute to ρ^0 production from transverse photons.

In Ref. [16], numerical predictions for the ratio $A_1^\rho/A_1^{\gamma^*p}$ were made for lepton beam energies of 15 GeV and 50 GeV. From these predictions, a ratio $A_1^\rho/A_1^{\gamma^*p}$ of about 2 can be interpolated for

the HERMES beam energy of 27.56 GeV i.e. at $\langle W \rangle = 4.9$ GeV. With a value of $A_1^{\gamma^*p}(x=0.07) = 0.13$, obtained from a parameterisation of the inclusive asymmetry measured at HERMES [32], a ratio $A_1^\rho/A_1^{\gamma^*p} = 1.9 \pm 0.8$ is inferred from the data, where the uncertainty is determined from the statistical uncertainty of A_1^ρ . This result is consistent with the above theoretical prediction that was made a quarter of a century before the data became available.

The ratio $A_1^\rho/A_1^{\gamma^*p}$ also has another interpretation if certain assumptions are made. The two processes are schematically shown in Fig. 4. As

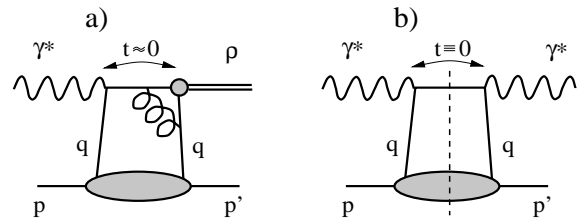


Figure 4: Schematic graphs for exclusive ρ^0 production (a) and inclusive lepton-nucleon scattering (b).

already mentioned, only transverse photons can contribute to the double-spin asymmetries A_1^ρ and $A_1^{\gamma^*p}$. For transverse photons both asymmetries can be expressed in terms of s -channel helicity amplitudes as

$$A_1^\rho = \frac{|f_{++}^{++}|^2 - |f_{++}^{--}|^2}{|f_{++}^{++}|^2 + |f_{++}^{--}|^2}, \quad A_1^{\gamma^*p} = \frac{\text{Im} f_{++}^{++} - \text{Im} f_{++}^{--}}{\text{Im} f_{++}^{++} + \text{Im} f_{++}^{--}}. \quad (9)$$

Here, $f_{ii}^{\alpha\alpha'}$ are the helicity-conserving ($\alpha = \alpha'$, $i = i'$) amplitudes with $i, i' = \pm 1/2$ the helicity of the incident and scattered nucleon, $\alpha = 0, \pm 1$ the helicity of the incident photon, and $\alpha' = 0, \pm 1$ the helicity of the outgoing photon or ρ^0 meson. Here it is assumed that the above helicity amplitudes for ρ^0 production and inclusive reactions differ only by a common factor, and that the contributions of helicity-flip amplitudes ($\alpha \neq \alpha'$, $i \neq i'$) are small and can be neglected. For the asymmetry in the cross section for ρ^0 production, the amplitudes have to be squared, while the expression for the asymmetry in the inclusive reaction

is based on the optical theorem. Assuming that f_{++}^{++} and f_{++}^{--} are primarily imaginary, as is the case for exclusive reactions at small x , the ratio $A_1^\rho/A_1^{\gamma^*p}$ can be approximated as

$$\frac{A_1^\rho}{A_1^{\gamma^*p}} \simeq \frac{2}{1 + (A_1^{\gamma^*p})^2}, \quad (10)$$

which is about 2 since the inclusive asymmetry at low x is of order 0.1.

In models based on perturbative QCD [9], diffractive ρ^0 production by longitudinal photons is described by three distinct components: a distribution amplitude for the meson, a hard scattering amplitude for the exchange of quarks and gluons, and a non-perturbative description of the target nucleon by skewed parton distributions (SPD's) allowing a sensitivity of the diffractive process to the internal (spin) structure of the nucleon. A general proof of the factorisation theorem in diffractive meson production, an important prerequisite for the definition of SPD's, exists only for *longitudinal* photons, and does not apply to the production of mesons from *transverse* photons [9,34]. As an important consequence, a clear interpretation of the asymmetry A_1^ρ within the framework of perturbative QCD and skewed parton distributions presently does not exist and would require substantial theoretical progress.

The present result indicating a non-zero double-spin asymmetry is in contrast to the preliminary result of a similar measurement by the SMC collaboration [33] at comparable values of Q^2 but at three times higher W , i.e. at smaller x . Their measurement of $A_{||}^\rho$ in several bins in Q^2 is consistent with zero, with a better statistical precision than the present measurement. In the context of Ref. [16] their $A_{||}^\rho$ is expected to be smaller since the asymmetries in inclusive deep-inelastic scattering decrease at the smaller values of x probed by the SMC measurement. Alternatively, at SMC the diffractive process is believed to be dominated by Pomeron or gluon exchange, whereas at the lower HERMES energy, there are indications that ρ^0 production is dominated by Reggeon or quark exchange [6,10]; the different asymmetry results of SMC and HERMES might well reflect the different production mechanisms in the two kinematic regimes.

In summary, evidence for a non-zero longitudinal double-spin asymmetry in the cross section for exclusive ρ^0 production in lepton-nucleon scattering has been observed. The value measured is $\langle A_1^\rho \rangle = 0.24 \pm 0.11_{\text{stat}} \pm 0.02_{\text{syst}}$, at $\langle W \rangle = 4.9$ GeV and $\langle Q^2 \rangle = 1.7$ GeV². No significant dependence on any kinematic variable was observed. A ratio $A_1^\rho/A_1^{\gamma^*p} = 1.9 \pm 0.8$ of the asymmetry in ρ^0 production to that in inclusive lepton-nucleon scattering was obtained. This result is consistent with an early prediction based on the generalised vector meson dominance model.

We gratefully acknowledge the DESY management for its support and the DESY staff and the staffs of the collaborating institutions. This work was supported by the FWO-Flanders, Belgium; the Natural Sciences and Engineering Research Council of Canada; the INTAS and TMR network contributions from the European Community; the German Bundesministerium für Bildung und Forschung; the Deutsche Forschungsgemeinschaft (DFG); the Deutscher Akademischer Austauschdienst (DAAD); the Italian Istituto Nazionale di Fisica Nucleare (INFN); Monbusho International Scientific Research Program, JSPS, and Toray Science Foundation of Japan; the Dutch Foundation for Fundamenteel Onderzoek der Materie (FOM); the U.K. Particle Physics and Astronomy Research Council; and the U.S. Department of Energy and National Science Foundation.

References

- [1] J.J. Sakurai, Ann. Phys. **11** (1960) 1, and Phys. Rev. Lett. **22** (1969) 981.
- [2] T.H. Bauer, R.D. Spital, D.R. Yennie and F.M. Pipkin, Rev. Mod. Phys. **50** (1978) 261.
- [3] D.G. Cassel *et al.*, Phys. Rev. **D24** (1981) 2787.
- [4] L.P.A. Haakman, A. Kaidalov and J.H.Koch, Phys. Lett. **B365** (1996) 411.
- [5] J.A. Crittenden, Springer Tracts in Modern Physics 140 (1997).

- [6] HERMES Collaboration, A. Airapetian *et al.*, Eur. Phys. J. **C17** (2000) 389.
- [7] A.V. Radyushkin, Phys. Lett. **B380** (1996) 417, and Phys. Rev. **D56** (1996) 5524.
- [8] X. Ji, Phys. Rev. **D55** (1997) 7114, and Phys. Rev. Lett. **78** (1997) 610.
- [9] J.C. Collins, L. Frankfurt and M. Strikman, Phys. Rev. **D56** (1997) 2982.
- [10] M. Vanderhaeghen, P.A.M. Guichon and M. Guidal, Phys. Rev. Lett. **80** (1998) 5064, and Phys. Rev. **D60** (1999) 094017.
- [11] ZEUS Collaboration, J.Breitweg *et al.*, Eur. Phys. J. **C2** (1998) 247.
- [12] H1 Collaboration, C. Adloff *et al.*, Eur. Phys. J. **C13** (2000) 371.
- [13] K. Schilling and G. Wolf, Nucl. Phys. **B61** (1973) 381.
- [14] H. Fraas, Ann. Phys. **87** (1974) 417.
- [15] H. Fraas, B.J. Read and D. Schildknecht, Nucl. Phys. **B86** (1975) 346, and Nucl. Phys. **B88** (1975) 301.
- [16] H. Fraas, Nucl. Phys. **B113** (1976) 532.
- [17] M. Vanttinen and L. Mankiewicz, Phys. Lett. **B434** (1998) 141, and Phys. Lett. **B440** (1998) 157.
- [18] HERMES Collaboration, K. Ackerstaff *et al.*, Nucl. Inst. Meth. **A417** (1998) 230.
- [19] A.A. Sokolov and I.M. Ternov, Sov. Phys. Doklady **8** (1964) 1203.
- [20] D.P. Barber *et al.*, Nucl. Instr. and Meth. **A 329** (1993) 79; A. Most, Proc. of the 12th International Symposium on High-Energy Spin Physics, edited by C.W. de Jager *et al.*, Amsterdam, The Netherlands, World Scientific (1997) 800.
- [21] J. Stewart, Proc. of the Workshop Polarised gas targets and polarised beams, edited by R.J. Holt and M.A. Miller, Urbana-Champaign, USA, AIP Conf. Proc. **421** (1997) 69.
- [22] HERMES Collaboration, K. Ackerstaff *et al.*, Phys. Rev. Lett. **82** (1999) 3025.
- [23] B. Anderson, G. Gustafson, G. Ingelman and T. Sjostrand, Z. Phys. **C9** (1981) 233.
- [24] T. Sjöstrand, Comp. Phys. Comm. **82** (1994) 74.
- [25] E665 Collaboration, M.R. Adams *et al.*, Z. Phys. **C74** (1997) 237.
- [26] L.W. Whitlow *et al.*, Phys. Lett. **B250** (1990) 193.
- [27] HERMES Collaboration, K. Ackerstaff *et al.*, Eur. Phys. Jour. C (in press), hep-ex/0002016.
- [28] E143 Collaboration, K. Abe *et al.*, Phys. Rev. **D58** (1998) 112003.
- [29] SMC Collaboration, D. Adams *et al.*, Phys. Rev. **D56** (1997) 5330.
- [30] F. Meissner, PhD Thesis, Humboldt University Berlin (2000), DESY-THESIS 2000-014.
- [31] I. Akushevich, Private Communication (1999).
- [32] HERMES Collaboration, A. Airapetian *et al.*, Phys. Lett. **B442** (1998) 484.
- [33] A. Tripet, Nucl. Phys. **B (Proc. Suppl.) 79** (1999) 529.
- [34] L. Mankiewicz and G. Piller, Phys. Rev. **D61** (1999) 074013.
- [35] S.J. Brodsky *et al.*, Phys. Rev. **D50** (1994) 3134.

Table 1: Results on asymmetries A_{\parallel}^{ρ} and A_{\perp}^{ρ} in exclusive ρ^0 production per kinematic bin.

Bin	$\langle Q^2 \rangle$ (GeV ²)	A_{\parallel}^{ρ}	A_{\perp}^{ρ}	$\langle \eta\sqrt{R} \rangle$
1	0.88	$0.102 \pm 0.070 \pm 0.007$	$0.195 \pm 0.154 \pm 0.017$	0.031
2	1.50	$0.116 \pm 0.070 \pm 0.008$	$0.251 \pm 0.184 \pm 0.021$	0.053
3	3.26	$0.140 \pm 0.095 \pm 0.010$	$0.312 \pm 0.268 \pm 0.027$	0.086
Bin	$\langle W \rangle$ (GeV)	A_{\parallel}^{ρ}	A_{\perp}^{ρ}	$\langle \eta\sqrt{R} \rangle$
1	4.35	$0.113 \pm 0.077 \pm 0.008$	$0.315 \pm 0.265 \pm 0.027$	0.076
2	4.87	$0.164 \pm 0.080 \pm 0.011$	$0.378 \pm 0.211 \pm 0.029$	0.052
3	5.50	$0.089 \pm 0.074 \pm 0.007$	$0.139 \pm 0.140 \pm 0.014$	0.032
Bin	$\langle -t' \rangle$ (GeV ²)	A_{\parallel}^{ρ}	A_{\perp}^{ρ}	$\langle \eta\sqrt{R} \rangle$
1	0.024	$0.101 \pm 0.079 \pm 0.007$	$0.198 \pm 0.197 \pm 0.018$	0.051
2	0.095	$0.119 \pm 0.073 \pm 0.008$	$0.244 \pm 0.184 \pm 0.021$	0.053
3	0.248	$0.137 \pm 0.079 \pm 0.010$	$0.288 \pm 0.199 \pm 0.024$	0.055
Bin	$\langle x \rangle$	A_{\parallel}^{ρ}	A_{\perp}^{ρ}	$\langle \eta\sqrt{R} \rangle$
1	0.032	$0.126 \pm 0.075 \pm 0.009$	$0.225 \pm 0.150 \pm 0.018$	0.026
2	0.059	$0.121 \pm 0.072 \pm 0.009$	$0.273 \pm 0.192 \pm 0.023$	0.049
3	0.119	$0.098 \pm 0.080 \pm 0.007$	$0.218 \pm 0.247 \pm 0.021$	0.085
Bin	$\langle \Phi/\pi \rangle$	A_{\parallel}^{ρ}	A_{\perp}^{ρ}	$\langle \eta\sqrt{R} \rangle$
1	-0.65	$0.064 \pm 0.078 \pm 0.005$	$0.103 \pm 0.189 \pm 0.013$	0.050
2	0.00	$0.123 \pm 0.076 \pm 0.009$	$0.269 \pm 0.203 \pm 0.023$	0.058
3	0.64	$0.166 \pm 0.076 \pm 0.011$	$0.352 \pm 0.186 \pm 0.028$	0.051
Bin	$\langle \phi/\pi \rangle$	A_{\parallel}^{ρ}	A_{\perp}^{ρ}	$\langle \eta\sqrt{R} \rangle$
1	-0.65	$0.085 \pm 0.079 \pm 0.006$	$0.157 \pm 0.194 \pm 0.016$	0.052
2	0.00	$0.005 \pm 0.080 \pm 0.003$	$-0.042 \pm 0.203 \pm 0.008$	0.055
3	0.65	$0.242 \pm 0.073 \pm 0.016$	$0.549 \pm 0.180 \pm 0.040$	0.053
Bin	$\langle \theta/\pi \rangle$	A_{\parallel}^{ρ}	A_{\perp}^{ρ}	$\langle \eta\sqrt{R} \rangle$
1	0.24	$0.181 \pm 0.074 \pm 0.012$	$0.391 \pm 0.180 \pm 0.030$	0.050
2	0.50	$0.153 \pm 0.081 \pm 0.011$	$0.342 \pm 0.211 \pm 0.027$	0.058
3	0.76	$0.026 \pm 0.075 \pm 0.004$	$0.014 \pm 0.185 \pm 0.009$	0.052
Bin	$\langle \Psi/\pi \rangle$	A_{\parallel}^{ρ}	A_{\perp}^{ρ}	$\langle \eta\sqrt{R} \rangle$
1	0.29	$0.052 \pm 0.078 \pm 0.005$	$0.078 \pm 0.197 \pm 0.011$	0.055
2	1.00	$0.154 \pm 0.075 \pm 0.011$	$0.325 \pm 0.183 \pm 0.026$	0.050
3	1.69	$0.159 \pm 0.078 \pm 0.010$	$0.321 \pm 0.195 \pm 0.026$	0.055